DYNAMICAL BARYON RESONANCES FROM CHIRAL UNITARITY

A. RAMOS

Departament d'Estructura i Constituents de la Matèria, Universitat de Barcelona, E-08028 Barcelona, Spain

C. BENNHOLD

Center for Nuclear Studies, Department of Physics, The George Washington University, Washington D.C. 20052

A. HOSAKA, T. HYODO

Research Center for Nuclear Physics, Osaka University, Ibaraki, Osaka 567-0047, Japan

D. JIDO

ECT*, Villa Tambosi, Strada delle Tabarelle 286, I-38050 Villazzano, Italy

U.-G. MEISSNER

HISKP, University of Bonn, Nußalle 14-16, D-53115 Bonn, Germany

J.A. OLLER

Departamento de Física, Universidad de Murcia, 30071 Murcia, Spain

E. OSET, M. J. VICENTE-VACAS

Departamento de Física Teórica and IFIC, Centro Mixto Universidad de Valencia-CSIC, Apartado 22085, E-46071 Valencia, Spain

We report on the latests developments in the field of baryonic resonances generated from the meson-baryon interaction in coupled channels using a chiral unitary approach. The collection of resonances found in different strangeness and isospin sectors can be classified into SU(3) multiplets. The $\Lambda(1405)$ emerges as containing the effect of two poles of the scattering amplitude and various reactions that might preferentially select one or the other pole are discussed.

2

1. Introduction

Establishing the nature of hadronic resonances is one of the primary goals in the field of hadronic physics. The interest lies in understanding whether they behave as genuine three quark states or they are dynamically generated through the iteration of appropriate non-polar terms of the hadron-hadron interaction, not being preexistent states that remain in the large N_c limit where the multiple scattering is suppressed. In the last decade, chiral perturbation theory (χPT) has emerged as a powerful scheme to describe low-energy meson-meson and meson-baryon dynamics. In recent years, the introduction of unitarity constraints has allowed the extension of the chiral description to much higher energies and, in addition, it has lead to the generation of many hadron resonances both in the mesonic and the baryonic sectors.

The $\Lambda(1405)$ resonance is a clear example of a dynamically generated state appearing naturally from the multiple scattering of coupled meson-baryon channels with strangeness $S = -1$ [1–5]. Recently, the interest in studying its properties has been revived by the observation in the chiral models that the nominal $\Lambda(1405)$ is in fact built up from two poles of the T-matrix in the complex plane [5–7] both contributing to the invariant $\pi\Sigma$ mass distribution, as it was the case within the cloudy bag model [8]. The fact that these two poles have different widths and partial decay widths into $\pi\Sigma$ and $\bar{K}N$ states opens the possibility that they might be experimentally observed in hadronic or electromagnetic reactions.

The unitary chiral dynamical models have been extended by various groups [5,7,9–16], covering an energy range of about 1.4–1.7 GeV and giving rise to a series of resonant states in all isospin and strangeness sectors. All these observations have finally merged into the classification of the dynamical generated baryon resonances into SU(3) multiplets [17], as seen also in Ref. [18].

In this contribution we present a summary of our latest developments in the field of baryon resonances generated from chiral unitary dynamics.

2. Meson-baryon scattering model

The search for dynamically generated resonances proceeds by first constructing the meson-baryon coupled states from the octet of ground state positive-parity baryons (B) and the octet of pseudoscalar mesons (Φ) for a

given strangeness channel. Next, from the lowest order lagrangian

$$L_1^{(B)} = \langle \bar{B} i \gamma^\mu \frac{1}{4f^2} [(\Phi \partial_\mu \Phi - \partial_\mu \Phi \Phi) B - B(\Phi \partial_\mu \Phi - \partial_\mu \Phi \Phi)] \rangle \qquad (1)$$

one derives the driving kernel in s-wave

$$V_{ij} = -C_{ij} \frac{1}{4f^2} (2\sqrt{s} - M_i - M_j) \left(\frac{M_i + E_i}{2M_i} \right)^{1/2} \left(\frac{M_j + E_j}{2M_j} \right)^{1/2} , \qquad (2)$$

where the constants C_{ij} are SU(3) coefficients encoded in the chiral lagrangian and f is the meson decay constant, which we take to have an average value of $f = 1.123 f_\pi$, where $f_\pi = 92.4$ MeV is the pion decay constant. While at lowest order in the chiral expansion all the baryon mases are equal to the chiral mass M_0, the physical masses are used in Eq. (2) as done in Refs. [4,12]. We recall that, in addition to the Weinberg-Tomozawa or seagull term of Eq. (2), one also has at the same order of the chiral expansion the direct and exchange diagrams considered in Ref. [5]. Their contribution increases with energy and represents around 20% of that from the seagull term at $\sqrt{s} \simeq 1.5$ GeV.

The scattering matrix amplitudes between the various meson-baryon states are obtained by solving the coupled channel equation

$$T_{ij} = V_{ij} + V_{il} G_l T_{lj} , \qquad (3)$$

where i, j, l are channel indices and the V_{il} and T_{lj} amplitudes are taken on-shell. This is a particular case of the N/D unitarization method when the unphysical cuts are ignored [19,20]. Under these conditions the diagonal matrix G_l is simply built from the convolution of a meson and a baryon propagator and can be regularized either by a cut-off ($q_{\max}^l$), as in Ref. [4], or alternatively by dimensional regularization depending on a subtraction constant (a_l) coming from a subtracted dispersion relation [5,12].

3. Strangeness $S = -1$

In the case of $K^- p$ scattering, we consider the complete basis of meson-baryon states, namely $K^- p$, $\bar{K}^0 n$, $\pi \Lambda$, $\eta \Lambda$, $\eta \Sigma^0$, $\pi^+ \Sigma^-$, $\pi^- \Sigma^+$, $\pi^0 \Sigma^0$, $K^+ \Xi^-$ and $K^0 \Xi^0$, thus preserving SU(3) symmetry in the limit of equal baryon and meson masses. Taking a cut-off of 630 MeV, the scattering observables, threshold branching ratios and properties of the $\Lambda(1405)$ resonance were well reproduced [4,11], as shown in Table 1 and Figs. 1 and 2. The inclusion of the $\eta \Lambda, \eta \Sigma$ channels was found crucial to obtain a good agreement with experimental data in terms of the lowest order chiral lagrangian.

4

Table 1. Branching ratios at K^-p threshold. Experimental values taken from Refs. [21, 22].

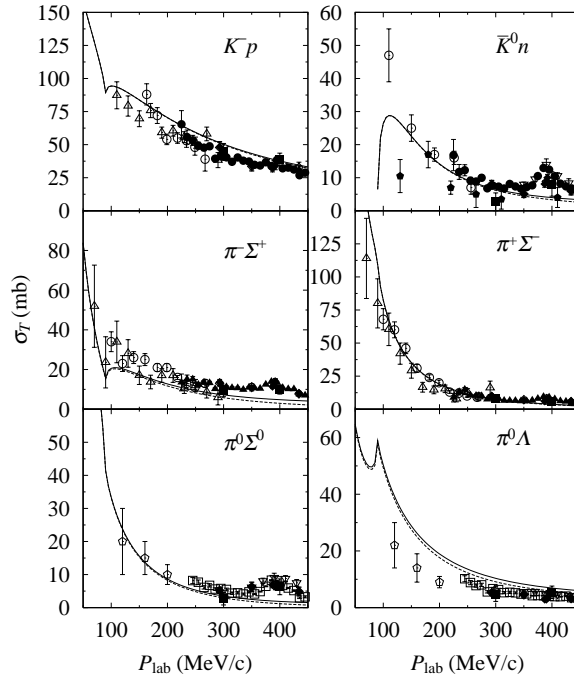| Ratio	Exp.	Model
$\gamma = \frac{\Gamma(K^-p \to \pi^+\Sigma^-)}{\Gamma(K^-p \to \pi^-\Sigma^+)}$	2.36 ± 0.04	2.32
$R_c = \frac{\Gamma(K^-p \to \text{charged particles})}{\Gamma(K^-p \to \text{all})}$	0.664 ± 0.011	0.627
$R_n = \frac{\Gamma(K^-p \to \pi^0\Lambda)}{\Gamma(K^-p \to \text{all neutral states})}$	0.189 ± 0.015	0.213

Figure 1. Total cross sections of the K^-p elastic and inelastic scatterings. The solid line denotes our results including both s-wave and p-wave. The dashed line shows our results without the p-wave amplitudes. The data are taken from Ref. [23].

Our model extrapolated smoothly to high energies [12] by using the dimensional regularization scheme. The subtraction constants resulted to have a "natural" size [5] which permits qualifying the generated resonances as being dynamical. While the $I = 0$ components of the $\bar{K}N \to \bar{K}N$ and
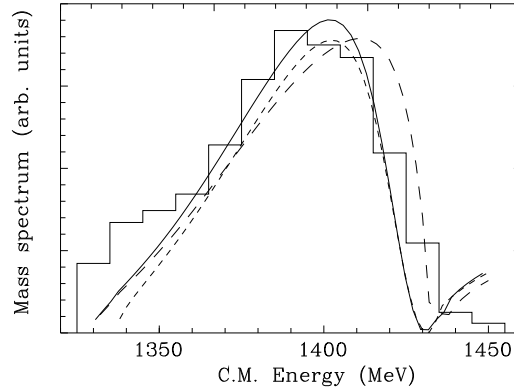
Figure 2. The $\pi\Sigma$ invariant mass distribution around the $\Lambda(1405)$ resonance. Results in particle basis (solid line), isospin basis (short-dashed line) or omitting the $\eta\Lambda$, $\eta\Sigma^0$ channels. Experimental histogram taken from Ref. [24].

Table 2. Pole positions and couplings to meson-baryon states of the dynamically generated resonances in the $S = -1$ sector [12].

	z_R (MeV)		$\mid g_{\pi\Sigma}\mid^2$	$\mid g_{\bar{K}N}\mid^2$	$\mid g_{\eta\Lambda}\mid^2$	$\mid g_{K\Xi}\mid^2$
$\Lambda(1405)$	1390−i66		8.4	4.5	0.59	0.38
	1426−i16		2.3	7.4	2.0	0.12
$\Lambda(1670)$	1680−i20		0.01	0.61	1.1	12
		$\mid g_{\pi\Lambda}\mid^2$	$\mid g_{\pi\Sigma}\mid^2$	$\mid g_{\bar{K}N}\mid^2$	$\mid g_{\eta\Sigma}\mid^2$	$\mid g_{K\Xi}\mid^2$
$\Sigma(1620)$	1579−i274	4.2	7.2	2.6	3.5	12

$\bar{K}N \to \pi\Sigma$ amplitudes displayed a clear signal from the $\Lambda(1670)$ resonance, the $I = 1$ amplitudes showed to be smooth and featureless without any trace of resonant behavior, in line with the experimental observation. In Table 2 we display the value of the poles of the scattering amplitude in the second Riemann sheet, $z_R = M_R - \mathrm{i}\Gamma/2$, together with the corresponding couplings to the various meson-baryon states, obtained from identifying the amplitudes T_{ij} with $g_i g_j/(z - z_R)$ in the limit $z \to z_R$. Two poles define the $\Lambda(1405)$ resonance. The pole at lower energy is wider and couples mostly to $\pi\Sigma$ states, while that at higher energy is narrower and couples mostly to $\bar{K}N$ states. The consequences of this two-pole nature of the $\Lambda(1405)$ are discussed in detail in Refs. [17,25]. We also find poles corresponding to the $\Lambda(1670)$ and $\Sigma(1620)$ resonances. The large coupling of the $\Lambda(1670)$ to $K\Xi$ states allows one to identify this resonance as a "quasibound" $K\Xi$ state. The large width associated to the $\Sigma(1620)$ resonance, rated as 1-star by the Particle Data Group (PDG) [26], explains why there is no trace of

6

this state in the scattering amplitudes.

4. Strangeness $S = -2$

The unitariy chiral meson-baryon approach has also been extended to the $S = -2$ sector [13] to investigate the nature of the lowest possible s-wave Ξ states, the $\Xi(1620)$ and $\Xi(1690)$, rated 1- and 3-star, respectively, and quoted with unknown spin and parity by the PDG [26]. Allowing the subtraction constants to vary around a natural size of -2, a pole is found at $z_R = 1605 - i66$, the real part showing a strong stability against the change of parameters. The imaginary part would apparently give a too large width of 132 MeV compared to the experimental ones reported to be of 50 MeV or less. However, due a threshold effect, the actual $\pi\Xi$ invariant mass distribution, displayed in Fig. 3, shows a much narrower width and resembles the peaks observed experimentally.
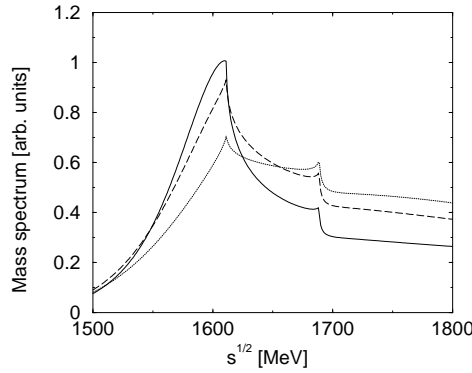

Figure 3.   The $\pi\Xi$ invariant mass distribution as a function of the center-of-mass energy, for several sets of subtraction constants. Solid line: $a_{\pi\Xi} = -3.1$ and $a_{\bar{K}\Lambda} = -1.0$; Dashed line: $a_{\pi\Xi} = -2.5$ and $a_{\bar{K}\Lambda} = -1.6$; Dotted line: $a_{\pi\Xi} = -2.0$ and $a_{\bar{K}\Lambda} = -2.0$. The value of the two other subtraction constants, $a_{\bar{K}\Sigma}$ and $a_{\eta\Xi}$, is fixed to -2.0 in all curves.

The couplings obtained are $\mid g_{\pi\Xi} \mid^2 = 5.9$, $\mid g_{\bar{K}\Lambda} \mid^2 = 7.0$, $\mid g_{\bar{K}\Sigma} \mid^2 = 0.93$ and $\mid g_{\eta\Xi} \mid^2 = 0.23$. The particular large values for final $\pi\Xi$ and $\bar{K}\Lambda$ states rule out identifying this resonance with the $\Xi(1690)$, which is found to decay predominantly to $\bar{K}\Sigma$ states. Therefore, the dynamically generated $S = -2$ state can be safely identified with the $\Xi(1620)$ resonance and this also allows us to assign the values $J^P = 1/2^-$ to its unmeasured spin and parity. The model of Ref. [18] finds this state at $z_R = 1565 - i124$, together

with another pole at $z_R = 1663 - \mathrm{i}2$, identified with the $\Xi(1690)$ because of its strong coupling to $\bar{K}\Sigma$ states.

5. Strangeness $S = 0$

For completeness, we briefly mention here the work done in the $S = 0$ sector [9,10] where the $N(1535)$ was generated dynamically within the same approach. In order to reproduce the phase shifts and inelasticities, four subtraction constants were adjusted to the data leading to a $N(1535)$ state with a total decay width of $\Gamma \simeq 110$ MeV, divided into $\Gamma_\pi \simeq 43$ MeV and $\Gamma_\eta \simeq 67$ MeV, compatible with present data within errors. The dynamical $N(1535)$ is found to have strong couplings to the $K\Sigma$ and ηN final states.

6. SU(3) multiplets of resonant states

The SU(3) symmetry encoded in the chiral lagrangian permits classifying all these resonances into SU(3) multiplets. We first recall that the meson-baryon states built from the octet of pseudoscalar mesons and the octet of ground state baryons can be classified into the irreducible representations:

$$8 \otimes 8 = 1 \oplus 8_s \oplus 8_a \oplus 10 \oplus \overline{10} \oplus 27 \qquad (4)$$

Taking a common meson mass and a common baryon mass, the lowest-order meson-baryon chiral lagrangian is exactly SU(3) invariant. If, in addition, all the subtraction constants a_l are equal to a common value, the scattering problem decouples into each of the SU(3) sectors. Using SU(3) Clebsh-Gordan coefficients, the matrix elements of the transition potential V in a basis of SU(3) states are

$$V_{\alpha\beta} \propto -\frac{1}{4f^2} \sum_{i,j} \langle i, \alpha \rangle C_{ij} \langle j, \beta \rangle = \frac{1}{4f^2} \mathrm{diag}(-6, -3, -3, 0, 0, 2) \,, \qquad (5)$$

taking the following order for the irreducible representations: $1,8_s,8_a,10,\overline{10}$ and 27. The attraction in the singlet and the two octet channels gives rise to bound states in the unitarized amplitude, with the two octet poles being degenerate [17]. By breaking the SU(3) symmetry gradually, allowing the masses and subtraction constants to evolve to their physical values, the degeneracy is lost and the poles move along trajectories in the complex plane as shown in Fig. 4, which collects the behavior of the $S = -1$ states. As discussed further in Refs. [17,25], two poles in the $I = 0$ sector appear very close in energy and they will manifest themselves as a single resonance, the $\Lambda(1405)$, in invariant $\pi\Sigma$ mass distributions.
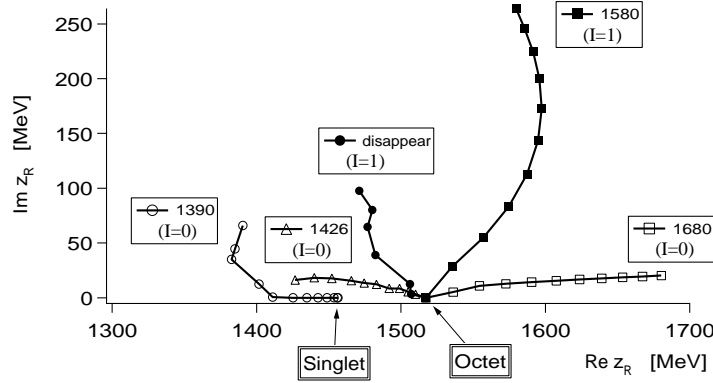
8

Figure 4. Trajectories of the poles in the scattering amplitudes obtained by changing the SU(3) breaking parameter x gradually. At the SU(3) symmetric limit ($x = 0$), only two poles appear, one is for the singlet and the other (two-times degenerate) for the octets. The symbols correspond to the step size $\delta x = 0.1$. The results are from Ref. [17].

7. The two-pole nature of the $\Lambda(1405)$

The $\Lambda(1405)$ is seen through the invariant mass distributions of $\pi\Sigma$ states given by

$$\frac{d\sigma}{dM_I} = |\sum_i C_i t_{i\to\pi\Sigma}|^2 p_{CM} \tag{6}$$

with i standing for any of the coupled channels ($\bar{K}N$, $\pi\Sigma$, $\eta\Lambda$, $K\Xi$) and C_i being coefficients that determine the strength for the excitation of channel i, which eventually evolves into a $\pi\Sigma$ state through the multiple scattering. As the two $\Lambda(1405)$ poles couple differently to $\pi\Sigma$ and $\bar{K}N$ states, the amplitudes $t_{\pi\Sigma\to\pi\Sigma}$, $t_{\bar{K}N\to\pi\Sigma}$ are dominated by one or the other pole, respectively, thus making the invariant mass distribution sensitive to the coefficients $C_{\pi\Sigma}$, $C_{\bar{K}N}$, *i.e.* to the reaction used to generate the $\Lambda(1405)$.

An interesting example is found in the radiative production reaction $K^-p \to \gamma\Lambda(1405)$. In order to access the subthreshold region, the photon must be radiated from the initial K^-p state, ensuring that the $\Lambda(1405)$ resonance is initiated from K^-p states, hence selecting the pole that couples more strongly to $\bar{K}N$ which is narrower and appears at a higher energy. The calculated invariant mass $\pi\Sigma$ distribution [27] appears indeed displaced to higher energies (~ 1420 MeV) and it is narrower (35 MeV) than what one obtains from other reactions.
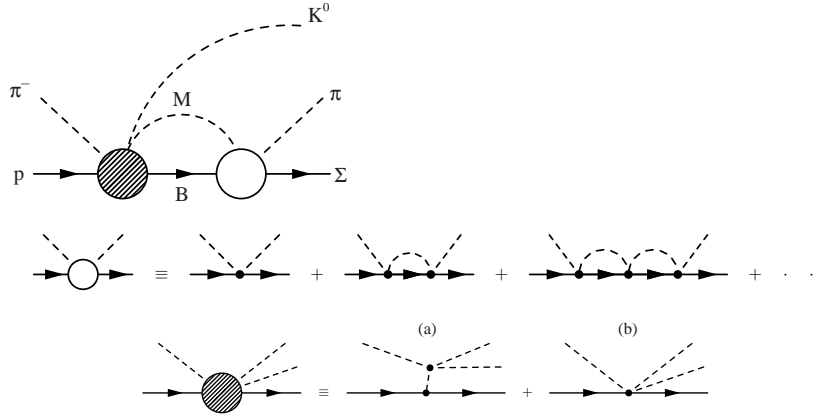
Figure 5.   Diagrams entering the production of the $\Lambda(1405)$ in the reaction $\pi^- p \to K^0 \Lambda(1405) \to K^0 \pi \Sigma$.

The $\Lambda(1405)$ can also be produced from the reaction (γ, K^+) on protons, recently implemented at LEPS of SPring8/RCNP [28]. In this case, the invariant mass distribution of the final meson-baryon state obtained in Ref. [29] shows a width of around 50 MeV. Due to the particular isospin decomposition of the $\pi\Sigma$ states, the $\pi^-\Sigma$ and $\pi^+\Sigma^-$ cross sections differ in the sign of the interference between $I = 0$ and $I = 1$ amplitudes (omitting the negligible $I = 2$ contribution). This difference has been observed in the experiment performed at SPring8/RCNP [28] and provides some information on the $I = 1$ amplitude.

The dynamics that goes into the $\pi^- p \to K^0 \pi \Sigma$ reaction, from which the experimental data of the $\Lambda(1405)$ resonance have been extracted [30], has recently been investigated [31]. As shown in Fig. 5, the process is separated into a part which involves tree level $\pi^- p \to K^0 MB$ amplitudes (hatched blob), and a second part which involves the final state interaction $MB \to \pi\Sigma$. The initial process is described following the model for the $\pi N \to \pi\pi N$ reaction close to threshold, which contains a pion pole term and a contact term, both of them calculated from the chiral lagrangians.

Since in this reaction $\sqrt{s} \sim 1900$ MeV, one must also consider resonance excitation in the πN collision leading to the decay of the resonance in MMB, as seen in Fig. 6. We select the $N^*(1710)$ since, in the energy region of interest, it is the only $S = 0$ P_{11} resonance with the same quantum numbers of the nucleon having a very large branching ratio to $\pi\pi N$ (40-90%) [26].

10
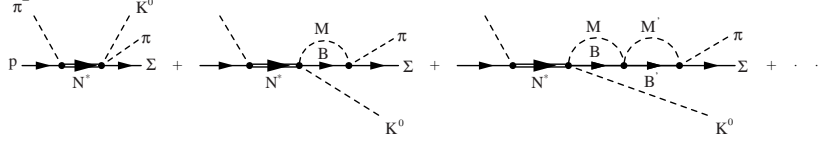
Figure 6.   Resonant mechanisms for $\Lambda(1405)$ production in the $\pi^- p \to K^0 \pi \Sigma$ reaction.
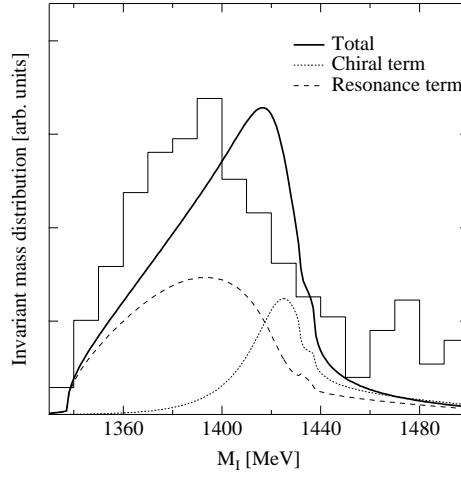
Figure 7.   Invariant mass distribution of $\pi\Sigma$ obtained by averaging $\pi^+\Sigma^-$ and $\pi^-\Sigma^+$. The histogram shows the experimental data taken from Ref. [30]. Resonance parameters: $M_R = 1740$, $\Gamma_{N^*} = 200$ MeV, $\Gamma_{\pi N} = 30$ MeV and $\Gamma_{\pi\pi N} = 120$ MeV.

The contribution of the chiral and resonant mechanisms to the invariant mass distribution are shown in Fig. 7 by the dotted and dashed lines, respectively. Both contributions are of similar size and their coherent sum (solid line) produces a distribution more in agreement with the experimental histogram. The chiral tree amplitude $\pi^- p \to K^0 M_i B_i$ for the case $M_i B_i = \bar{K} N$ involves the combinations $3F - D$ and $D + F$, which are large compared to the $D - F$ combination that one finds for $M_i B_i \equiv \pi\Sigma$ (we take $F = 0.51$ and $D = 0.75$). Therefore, the chiral distribution gives a larger weight to the $t_{\bar{K}N \to \pi\Sigma}$ amplitude, which is dominated by the narrower pole at higher energy. On the contrary, the the $N^* \to BM_1 M_2$ vertex in the resonant mechanism goes like the difference of energies of the outgoing mesons prior to final state interaction effects, which is practically zero for $N\bar{K}K^0$ and 300 MeV for $\Sigma\pi K^0$. Therefore, the resonant contribution is strongly

dominated by the $t_{\pi\Sigma\to\pi\Sigma}$ amplitude, which couples more strongly to the wider pole at lower energy.

Recently, the production of the $\Lambda(1405)$ through K^* vector meson photoproduction, $\gamma p \to K^*\Lambda(1405) \to \pi K \pi \Sigma$, using linearly polarized photons has been studied [32]. Selecting the events in which the polarization of the incident photon and that of the produced K^* are perpendicular, the mass distribution of the $\Lambda(1405)$ peaks at 1420 MeV, since in this case the process is dominated by t-channel K-meson exchange, hence selecting preferentially the $t_{\bar{K}N\to\bar{K}N}$ amplitude.

8. Summary and Conclusions

By implementing unitarity in the study of meson-baryon scattering using the lowest order chiral lagrangian, a series of resonant states have been dynamically generated in all strangeness and isospin sectors.

In the SU(3) limit, all these resonances belong to a singlet or to either of the two (degenerate) octets of dynamically generated poles of the SU(3) symmetric scattering amplitude.

In the physical limit, there are two $I = 0$ poles representing the $\Lambda(1405)$, the one at lower energy having a larger imaginary part than the one at higher energy. These poles couple differently to $\pi\Sigma$ and $\bar{K}N$ states and, as a consequence, the properties of the $\Lambda(1405)$ will depend on the particular reaction used to produce it. Various processes that might preferentially select the contribution from one or the other pole have been discussed.

Acknowledgments

References

1. M. Jones, R. H. Dalitz, and R. R. Horgan, Nucl. Phys. **B129**, 45 (1977).
2. N. Kaiser, P. B. Siegel and W. Weise, Nucl. Phys. **A594**, 325 (1995).
3. N. Kaiser, T. Waas and W. Weise, Nucl. Phys. **A612**, 297 (1997).
4. E. Oset and A. Ramos, Nucl. Phys. **A635**, 99 (1998).
5. J. A. Oller and U. G. Meissner, Phys. Lett. **B500**, 263 (2001).
6. D. Jido, A. Hosaka, J. C. Nacher, E. Oset, and A. Ramos, Phys. Rev. C **66**, 025203 (2002).

12

7. C. Garcia-Recio, J. Nieves, E. Ruiz Arriola, and M. J. Vicente Vacas, Phys. Rev. D **67**, 076009 (2003).
8. J. Fink, P. J., G. He, R. H. Landau, and J. W. Schnick, Phys. Rev. C **41**, 2720 (1990).
9. J. C. Nacher, A. Parreño, E. Oset, A. Ramos, A. Hosaka and M. Oka, Nucl. Phys. **A678**, 187 (2000).
10. T. Inoue, E. Oset and M. J. Vicente-Vacas, Phys. Rev. C **65**, 035204 (2002).
11. D. Jido, E. Oset, and A. Ramos, Phys. Rev. C **66**, 055203 (2002).
12. E. Oset, A. Ramos and C. Bennhold, Phys. Lett. **B527**, 99 (2002).
13. A. Ramos, E. Oset and C. Bennhold, Phys. Rev. Lett. **89**, 252001 (2002).
14. J. Nieves and E. Ruiz Arriola, Nucl. Phys. **A679**, 57 (2000);
15. J. Nieves and E. Ruiz Arriola, Phys. Rev. D **64**, 116008 (2001)
16. M. F. M. Lutz and E. E. Kolomeitsev, Nucl. Phys. **A700**, 193 (2002).
17. D. Jido, J. A. Oller, E. Oset, A. Ramos and U. G. Meissner, Nucl. Phys. **A725**, 181 (2003).
18. C. García-Recio, M. F. M. Lutz and J. Nieves, Phys. Lett. **B582** (2004) 49.
19. J. A. Oller and E. Oset, Phys. Rev. D **60**, 074023 (1999).
20. J. A. Oller and U.G. Meissner, Nucl. Phys. **A673**, 311 (2000).
21. D. N. Tovee *et al.*, Nucl. Phys. **B33**, 493 (1971).
22. R. J. Nowak *et al.*, Nucl. Phys. **B139**, 61 (1978).
23. J. Ciborowski *et al.*, J. Phys. **G8** (1982) 13; R. O. Bangerter *et al.*, Phys. Rev. D **23** (1981) 1484 ; T. S. Mast *et al.*, Phys. Rev. D **14** (1976) 13 ; M. Sakitt *et al.*, Phys. Rev. **139** (1965) B719 ; T. S. Mast *et al.*, Phys. Rev. D **11** (1975) 3078 ; P. Nordin, Jr, Phys. Rev. **123** (1961) 2168 ; D. Berley *et al.*, Phys. Rev. D **1** (1970) 1996 ; M. Ferro-Luzzi, R. D. Tripp, and M. B. Watson, Phys. Rev. Lett. **8** (1962) 28 ; M. B. Watson, M. Ferro-Luzzi, and R. D. Tripp, Phys. Rev. **131** (1963) 2248 ; P. Eberhard *et al.* Phys. Rev. Lett. **2** (1959) 312 ; J.K. Kim, Phys. Rev. Lett. **21** (1965) 719
24. R. J. Hemingway, Nucl. Phys. **B253**, 742 (1985).
25. D. Jido, J. A. Oller, E. Oset, A. Ramos and U. G. Meissner, these proceedings.
26. Particle Data Group, K. Hagiwara *et al.*, Phys. Rev. **D66**, 010001 (2002).
27. J. C. Nacher, E. Oset, H. Toki and A. Ramos, Phys. Lett. **B461**, 299 (1999).
28. J. K. Ahn, for the LEPS collaboration, Nucl. Phys. **A721**, 715c (2003).
29. J. C. Nacher, E. Oset, H. Toki and A. Ramos, Phys. Lett. **B455**, 55 (1999).
30. D. W. Thomas, A. Engler, H. E. Fisk, and R. W. Kraemer, Nucl. Phys. **B56**, 15 (1973).
31. T. Hyodo, A. Hosaka, E. Oset, A. Ramos and M. J. Vicente-Vacas, Phys. Rev. C **68**, 065203 (2003).
32. T. Hyodo, A. Hosaka, M. J. Vicente-Vacas and E. Oset, Phys. Lett. **B593**, 75 (2004).